# Stability properties of the monochromatic spectrum in a double-cavity laser

Alejandro A. Duarte and Hernán G. Solari
*Departamento de Física, FCEN, Universidad de Buenos Aires, Buenos Aires, Argentina*
(Received 9 October 1998; revised manuscript received 7 April 1999)

We discuss the process by which the spectrum of monochromatic modes of the laser in a double-cavity laser changes from that proper to a short cavity into that proper to a long cavity as the reflectivity of the ''external'' mirror is varied from 0 to 1. This work is the natural continuation of our previous work [Phys. Rev. A **58**, 614 (1998)], where the bifurcations occurring during this metamorphosis were studied. The transformation is mostly dictated by the boundary conditions and occurs regardless of the laser model. This transition is beyond the possibilities of simpler double-cavity laser models, such as those of Lang and Kobayashi [IEEE J. Quantum Electron. **QE-16**, 347 (1980)]. The stability properties of the monochromatic modes are studied as a function of the reflectivity of the external mirror *R*, the external cavity length *L*, and the applied current *J*. It is shown that for reflectivity values corresponding to the metamorphosis of the spectrum, by varying *J* and/or *R*, the system can give rise to a Hopf instability that involves the excitation of a roughly discrete set of frequencies. Note that these features are also beyond the possibilities of simpler models. We also discuss the role played by noise and show that it is possible for the system to show a high degree of susceptibility to noise, depending on *J*. [S1050-2947(99)10608-5]

PACS number(s): 42.55.Px, 47.20.Ky, 42.65.−k

## I. INTRODUCTION

The study of the spatiotemporal behavior of extended systems has recently been the subject of several theoretical and experimental investigations [1]. In this kind of system, the role played by the boundary conditions is very important because the number of effectively interacting modes depends mostly on the geometric characteristics rather than the physical processes occurring in the system. Therefore an understanding of the behavior of such systems with respect to the boundary conditions is a central problem in nonlinear dynamics. In this paper we study the changes affecting the monochromatic solutions of a laser with optical reinjection as a function of the boundary condition controlling the strength of the optical feedback. In particular, our study is focused on the stability properties of such solutions as a function of the boundary conditions.

The laser with optical reinjection has been the subject of intense research during the last decade, partly because the origin of the dynamical regimes appearing in this system is not fully understood from the academic point of view, and also because of its potential applications. In any case, the variety of dynamical phenomena present in this system has attracted much attention. It has been experimentally shown that they exhibit a variety of interesting dynamical states induced by feedback such as ''low-frequency fluctuations'' [2,3] and ''coherent collapse'' [3–6].

In this paper we consider a laser (semiconductor) of length $l$ ($l\sim 10$–$300$ $\mu$m) with an external mirror of reflectivity $R$ located at a distance $L$ ($L \gg l$), conforming in such a form a ''double-cavity laser'' [2–8]. While $R$ and $L$ are the control parameters controlling the boundary conditions, the gain of the active media depends on the pumping current $J$, which is the other control parameter.

The theoretical description of this system has been performed mainly through perturbative solutions valid only for limit cases, $R\sim 0$ [3–7] or $R\sim 1$ [8]. For $R\sim 0$, the laser is assumed to operate in a single (longitudinal) mode, so that the interesting variation is in time rather than space. The Lang-Kobayashi equations [7] are the paradigmatic model for this limit case.

Recently, a model that avoids the usual simplifications was presented [9]. On the one hand, the semiconductor media was considered in its full spatial extension, hence allowing for ''longitudinal multimode'' operation. On the other hand, the reinjected electromagnetic field was considered via the usual boundary conditions in the external mirror and the semiconductor-vacuum interface. The resulting model is a set of partial differential equations (PDE's) with time-delayed boundary conditions.

Following this approach, we were able to identify the changes occurring in the spectrum of the laser as $R$ was increased from 0 to 1 [9]. As expected, for $R=0$ the spectrum consists of a set of modes whose frequency separation is given by the length of the semiconductor ($\Delta\omega \propto 1/l$). For $R\sim 0$ the spectrum consists of clusters (islands) of solutions around each of the solitary laser modes. When $R$ is further increased, a drastic metamorphosis of the spectrum takes place: the islands are progressively absorbed into a larger one that progressively invades the spectrum from the low-frequency side. As $R$ is further increased, this island finally gains the whole frequency range of interest. In this case, the physically relevant part of the spectrum, the lower part of this large island, gives a wavy appearance reflecting the original islands, but the frequency separation between adjacent modes is dictated mainly by the length of the external cavity ($\Delta\omega \propto 1/L$). Further increasing $R$, the wavy appearance disappears until no trace of the original spectrum is found for $R\sim 1$. This transformation, which is mediated by an unusual sequence of bifurcations completely ruled by the boundary conditions [9], is the result of the competition between the cavities of length $l$ and $L$. Interestingly, this metamorphosis occurs regardless of the details of the susceptibility model; however, some of its features are model

 

dependent. Also note that this phenomenon is beyond the possibilities of the Lang-Kobayashi model.

The rest of the work is organized as follows: Sec. II formulates the problem as a nonlinear eigenvalue problem in laser physics; Sec. III discusses how the monochromatic modes are found and how the transformation of the spectrum takes place; Sec. IV describes how to perform the stability analysis; Sec. V presents the results obtained by performing the stability analysis; and finally Sec. VI presents the concluding remarks.

## II. LASER WITH OPTICAL FEEDBACK

In this section we present the description of the double-cavity laser. We consider a laser that extends in the $x$ direction, the active media are located at $0 \leqslant x \leqslant l$, while the external mirror of reflectivity $R$ is placed at $x=-L$. The dependence of the fields on the transversal coordinates $y$ and $z$ is neglected in what follows; hence the laser is described by the electric field $E(x,t)$, the polarization $P(x,t)$ [$P(x,t)=0$ for $-L \leqslant x \leqslant 0$], and the carrier density $N(x,t)$. Note that $P(x,t)=0$ and $N(x,t)=0$ for $-L \leqslant x \leqslant 0$.

For the sake of simplicity we consider the dimensionless form of the equations and field. The following factors, $ig(\gamma_\parallel/\gamma_\perp)^{1/2}N_T/2$, and $\hbar(\gamma_\parallel\gamma_\perp)^{1/2}/(2g)$, have been scaled out of the fields $P$ and $E$. In this case, the Maxwell equations read

$$\frac{\partial^2 E(x,t)}{\partial x^2}-\frac{\partial^2 E(x,t)}{\partial t^2}=i\beta\frac{\partial^2 P(x,t)}{\partial t^2}, \tag{1}$$

where $\beta=g^2N_T/\epsilon_0\hbar\gamma_\perp$, $g$ is the electric-dipole element of the material media ($g/e=0.20$ Å); time and distance are measured in units of the inverse of the polarization decay rate $\gamma_\perp$ ($\sim 10^{13}$ Hz) and $c\gamma_\perp^{-1}$, respectively. The material field $N$ is measured in units of a typical value $N_T=10^{24}m^{-3}$, and satisfies

$$\frac{\partial_\perp}{\partial_\parallel}\frac{\partial N(x,t)}{\partial t}=-N(x,t)+J+D\Delta N(x,t)+\frac{1}{2}[E(x,t)P^*(x,t)+E^*(x,t)P(x,t)], \tag{2}$$

where the different variables and operators have the following meaning: $J$ is the current pumping the carriers, $D$ is the diffusion coefficient for carriers, $\Delta N$ is the Laplacian of $N$, and $\gamma_\parallel$ is the nonradiative decay rate for the carrier density ($\sim 10^9$ Hz).

The boundary conditions complete our set of equations. They are the following: The electric field vanishes at the (perfect) mirror

$$E(l,t)=0; \tag{3}$$

the carriers cannot leave the semiconductor

$$\partial N(x,t)/\partial x|_{x=l}=\partial N(x,t)/\partial x|_{x=0}; \tag{4}$$

the electric and the magnetic fields are continuous (assuming that the semiconductor presents no magnetic polarization),

$$\lim_{\epsilon\to 0}E(-\epsilon,t)=\lim_{\epsilon\to 0}E(\epsilon,t), \tag{5}$$

$$\lim_{\epsilon\to 0}\partial E(x,t)/\partial x|_{x=-\epsilon}=\lim_{\epsilon\to 0}\partial E(x,t)/\partial x|_{x=\epsilon}; \tag{6}$$

the reflectivity of the external mirror is $R$. This condition has to be written in terms of the general solution of Maxwell's equation in the vacuum, $E(x,t)=H_+(t-x)+H_-(t+x)$, for $x\leqslant 0$, where $H$ is an arbitrary $C^2$ function. The condition reads

$$H_+(t+L)=-RH_-(t-L) \tag{7}$$

or $E(x,t)=-RH(t-\tau-x)+H(t+x)$, with $\tau=2L$. Note that having written the general solution for the electric field in $x\in[-L,0]$, we need to seek solutions to Eq. (1) only for $x\in[0,l]$. In this setting the problem becomes a partial differential equation with boundary conditions involving time delays [9].

In what follows we will further restrict our study to the case in which the diffusion of carriers is very fast; i.e., $D$ large in Eq. (2). Neglecting the spatial dependence of the carrier density $N(x,t)=N(t)$ in Eq. (2), we obtain

$$\frac{\partial_\perp}{\partial_\parallel}\frac{dN(t)}{dt}=-N(t)+J+\frac{1}{2l}\int_0^l dx[E(x,t)P^*(x,t)+E^*(x,t)P(x,t)]. \tag{8}$$

The approximation is compatible with the boundary conditions and implies disregarding the nonhomogeneous contributions to the carrier density as is customarily done [10,11]. It also implies that we are assuming that the decay rate of perturbations of the carrier density is fast compared with perturbations in the electromagnetic field and/or the polarization. A lesser degree of homogenization will increase the dynamical coupling of these perturbations. Actually, a strong dynamical coupling (slow diffusion) would make differentiating them meaningless since a perturbation of the fields will evolve into nonhomogeneous perturbations of the carrier density and vice versa.

The relation between the dimensionless variables $E$, $P$, and $N$ completes the equation set defining the characteristics of the active material. Under the assumption of a quadratic energy dependence (with respect to the electron wave vector) the following relation has been introduced in [12,13] for the dielectric susceptibility, $P(x,\omega)=\chi(\omega,N)E(x,\omega)$, as a function of the frequency $\omega$ and the carrier density $N(\omega)$,

$$\chi(\omega)=\Gamma\left(-\frac{1}{1-i\Omega}+C_1(\sqrt{\Omega+i}-iC_2)\right), \tag{9}$$

where $\Omega=\omega-\omega_g$ is the dimensionless detuning, $C_1=(2m\gamma_\perp/\hbar)^{3/2}/2\pi N_T$, and $C_2=2(2\hbar/\gamma_\perp ma^2)^{1/2}$. In this case, $\omega_g$ is the dimensionless frequency associated with the energy gap in the electronic bands of the semiconductor. The values adopted in numerical calculations are $\omega_g=235$, $\Gamma$

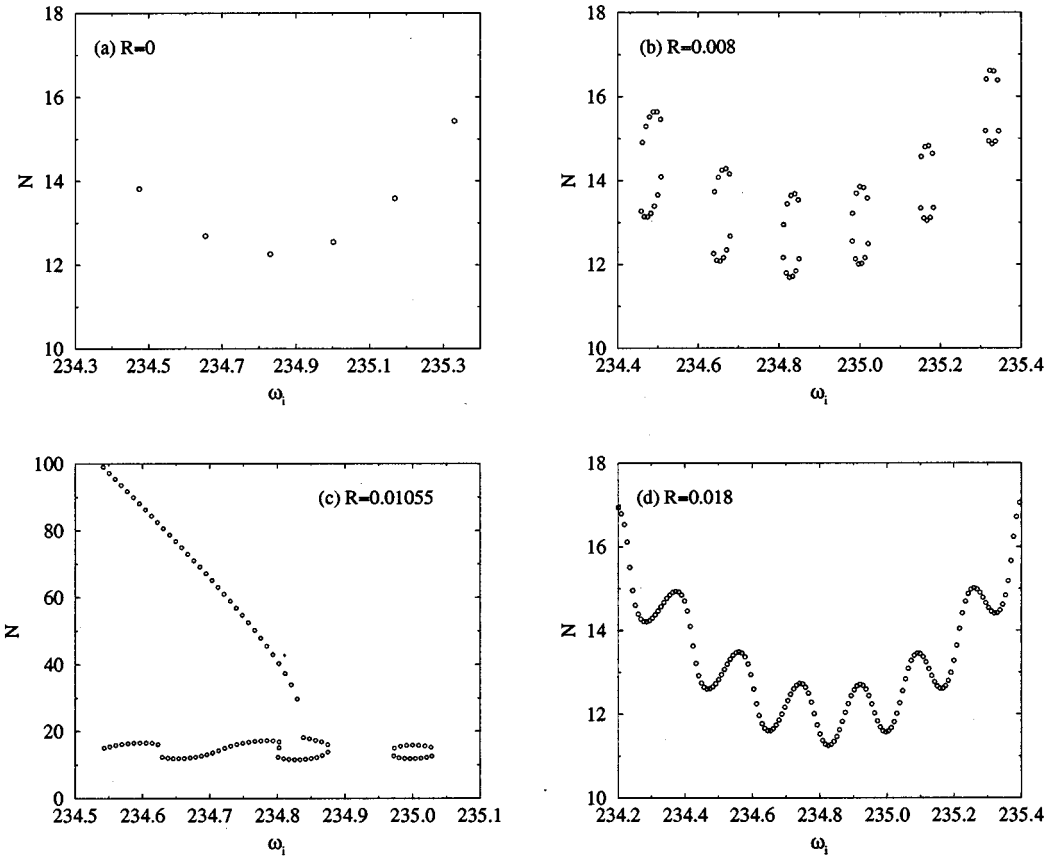


FIG. 1. Carrier density versus frequency for the laser with different levels of feedback strength: (a) $R=0$, (b) $R=0.008$, (c) $R=0.010\,55$, and (d) $R=0.018$.

$=0.4$, $C_1=11.4$, $C_2=9.6$, $l=10$, and $L=35l$. These values were taken from Ref. [13], and are in fact based on Refs. [10,14].

### III. MONOCHROMATIC SOLUTIONS

Monochromatic solutions are the simplest solutions of the laser system, both from the mathematical and physical points of view. They play the role of singularities [15] of the vector field in other dynamical systems and, together with their invariant manifolds, are the backbone of the dynamics of the laser. In this section we go through the changes suffered by the monochromatic spectrum in survey fashion of the results presented in Ref. [9] to give a broad picture of what happens when $R$ is increased from 0 to 1.

In Fig. 1(a) we show the monochromatic spectrum for $R=0$. The frequency separation of each mode from its adjacent modes is dictated by the semiconductor length ($\Delta\omega\propto 1/l$). The mode with minimal value of $N(\omega)$ is the stable (lasing) solution of the laser without optical reinjection (see Ref. [13] for a discussion). Note also that the Lang-Kobayashi equations [7] for $R=0$ present only this stable solution and are only valid in the vicinity of this solution. The spatial dependence of the solutions of this model is that of the reference mode. As $R$ is increased a few more monochromatic solutions are created through saddle-node bifurcations. These new solutions are clustered around the modes of the laser without optical reinjection in the $N(\omega)$ plot [see Fig. 1(b)], and we customarily refer to them as ''islands.'' The frequency separation between modes within an island is mainly dictated by the length of the external cavity ($\Delta\omega\propto 1/L$), while the frequency separation between adjacent islands is roughly the same as the frequency separation of the modes for $R=0$.

Further increasing $R$ changes the $N(\omega)$ drastically, Fig. 1(c). For low frequencies the islands have merged into one large island, while for high frequencies the structure of the modes still resembles a set of islands. These changes are the direct consequence of the bifurcations of solutions of the boundary equations discussed in Ref. [9].

The islands emerging from the stable solution of the laser without optical feedback approximately correspond to the solution of the Lang-Kobayashi equation (see Fig. 6 of [2] and Fig. 1 of [3]); but the description of the above metamorphosis is beyond the capabilities of this model. The reason for this is that these changes require the interaction in bifurcations of solutions coming from different islands, i.e., from different modes of the laser without feedback, and this possibility has been disregarded in the Lang-Kobayashi model.

For values of $R$ beyond the transition region, $R>0.011$, the spectrum of monochromatic modes is represented by a single wavy line [see Fig. 1(d)]. Increasing $R$ causes the waviness to disappear gradually. The resulting spectrum takes a form that closely resembles the situation for $R=1$.

### IV. LINEAR STABILITY ANALYSIS

In this section the linear stability analysis of the monochromatic solutions is presented. This is accomplished by the

usual methods, but special care is exercised to incorporate the boundary conditions in the description.

Within the active media the electric field, polarization, and carrier density are expanded in the form

$$\begin{aligned}E(x,t)=&\exp(-i\omega t)[F_+\exp(ikx)+F_-\exp(-ikx)]\\&+\exp[(\lambda-i\omega)t][A_+(x)\exp(ikx)\\&+A_-(x)\exp(-ikx)]+\exp[(\lambda^*-i\omega)t]\\&\times[B_+(x)\exp(ikx)+B_-(x)\exp(-ikx)],\end{aligned}$$

$$N(t)=N_0+X_n\exp(\lambda t)+X_n^*\exp(\lambda^* t),$$

where $F_\pm$, $N_0$, $\omega$, and $k$ are, respectively, the amplitudes, carrier density, frequency, and wave vector of the monochromatic solutions under consideration. Note that, since $E$ is not real, $A_+\neq A_-$, in principle, and $B_+\neq B_-$. Since the temporal dependence of the electric field is known, it is straightforward to compute the polarization using Eq. (9). The resulting linearized polarization is

$$\begin{aligned}P_L(x,t)=&\chi(\omega,N_0)\exp(-i\omega t)[F_+\exp(ikx)+F_-\exp(-ikx)]+\chi(\omega+i\lambda,N_0)\exp[(\lambda-i\omega)t][A_+(x)\exp(ikx)\\&+A_-(x)\exp(-ikx)]+\chi(\omega+i\lambda^*,N_0)\exp[(\lambda^*-i\omega)t][B_+(x)\exp(ikx)+B_-(x)\exp(-ikx)]\\&-\frac{\Gamma}{1-i\Omega}[F_+\exp(ikx)+F_-\exp(-ikx)]\{X_n\exp[(\lambda-i\omega)t]+X_n^*\exp[(\lambda^*-i\omega)t]\}.\end{aligned}$$

The linearized equations for the electric field under the assumption of a smooth and slowly varying envelope read

$$\pm\partial_x A_\pm=a(\lambda)A_\pm+F_\pm b(\lambda)X_n,$$

$$\pm\partial_x B_\pm=a(\lambda^*)B_\pm+F_\pm b(\lambda^*)X_n^*,$$

where

$$a(\lambda)=\frac{k^2+(\lambda-i\omega)^2[1+i\beta\chi(\omega+i\lambda,N_0)]}{2ik},$$

$$b(\lambda)=-\frac{\beta\Gamma(\lambda-i\omega)^2}{2k(1-i\Omega)}.$$

This set of equations has solutions of the form

$$A_\pm(x)=A_\pm^0\exp[\pm a(\lambda)x]-\frac{b(\lambda)}{a(\lambda)}F_\pm X_n,$$

$$B_\pm(x)=B_\pm^0\exp[\pm a(\lambda^*)x]-\frac{b(\lambda^*)}{a(\lambda^*)}F_\pm X_n^*.$$

So far we have only considered the expansion of the fields inside the semiconductor. The electric field in the external cavity can be expanded in the following form:

$$\begin{aligned}E(x,t)=&\exp(-i\omega t)h_0[\exp(-i\omega x)-R\exp(i\omega\tau)\exp(i\omega x)]\\&+\exp(-i\omega t)\\&\times[h(t+x)\exp(-i\omega x)\\&-R\exp(i\omega\tau)h(t-\tau-x)\exp(i\omega x)],\end{aligned}$$

where $h_0$ is the external field amplitude of the mode. While the boundary condition for $x=-L$ has been incorporated into the expansion of $H(x,t)$, the boundary conditions for $x=0$ and $x=l$ are considered separately. The boundary condition for $x=0$ imposes

$$\{1-R\exp[(i\omega-\lambda)\tau]\}X_h=A_+(0)+A_-(0),$$

$$\{1-R\exp[(i\omega-\lambda^*)\tau]\}Y_h=B_+(0)+B_-(0),$$

$$\begin{aligned}&(\lambda-i\omega)\{1+R\exp[(i\omega-\lambda)\tau]\}X_h\\&\quad=\partial_x A_+(0)+\partial_x A_-(0)+ik[A_+(0)-A_-(0)],\end{aligned}$$

$$\begin{aligned}&(\lambda^*-i\omega)\{1+R\exp[(i\omega-\lambda^*)\tau]\}Y_h\\&\quad=\partial_x B_+(0)+\partial_x B_-(0)+ik[B_+(0)-B_-(0)].\end{aligned}$$

with $h(t)=X_h\exp(\lambda t)+Y_h\exp(\lambda^* t)$.

On the other side of the semiconductor, $x=l$, the perfect mirror imposes

$$A_+^0=-A_-^0\exp\{-2[a(\lambda)+ik]l\},$$

$$B_+^0=-B_-^0\exp\{-2[a(\lambda^*)+ik]l\}.$$

The linearized version of Eq. (8) reads (after considering the boundary conditions)

$$\left(\frac{\lambda\partial_{\perp}}{\partial_{\parallel}}+1\right)X_n=[\hat{\chi}^*(\lambda^*)+\hat{\chi}(0)]\frac{1-\exp\{-2[a^*(\lambda^*)-2\,\mathrm{Im}(k)]l\}}{2[a^*(\lambda^*)-2\,\mathrm{Im}(k)]l}F_-B_-^{0\,*}$$
$$+[\hat{\chi}(\lambda)+\hat{\chi}(0)^*]\frac{1-\exp\{-2[a(\lambda)-2\,\mathrm{Im}(k)]l\}}{2[a(\lambda)-2\,\mathrm{Im}(k)]l}F_-^*A_-^0$$
$$-\left(\frac{2\Gamma}{1+\Omega^2}+[\hat{\chi}^*(\lambda^*)+\hat{\chi}(0)]\frac{b^*(\lambda^*)}{a^*(\lambda^*)}+[\hat{\chi}(\lambda)+\hat{\chi}^*(0)]\frac{b(\lambda)}{a(\lambda)}\right)\frac{\exp[4\,\mathrm{Im}(k)l]-1}{4\,\mathrm{Im}(k)l}|F_-|^2X_n,$$

where $\hat{\chi}(\lambda)\equiv\chi(\omega+i\lambda,N_0)$.

After considering all the equations, a system of five (linear, homogeneous, algebraic, complex) equations with five unknown complex numbers [$X_h$, $Y_h^*$, $A_-^0$, $(B_-^0)^*$, and $X_n$] can be obtained. This system only has nontrivial solutions if the determinant of the (associated) matrix is zero. Solving for $\lambda$ the implicit equation resulting from these considerations, we obtain the time dependence of the perturbations, $\lambda$.

## V. STABILITY PROPERTIES OF THE MONOCHROMATIC SOLUTIONS

In this section the stability properties of the monochromatic modes is considered while the control parameter space is explored through different cuts. Sections V A–V C, deal with the variation of $R$, $L$, and $J$, respectively. In any case, it is stated whether $R<R^*(\omega)$, $R\sim R^*(\omega)$, or $R>R^*(\omega)$, where $R^*(\omega)$ is the reflectivity value where the transition of the spectrum occurs for the frequency range under consideration.

### A. Linear stability as a function of the reflectivity of the mirror

The stability properties of the monochromatic solutions are studied as $R$ is increased from 0, while $J=40$. The effect of $R$ is twofold: (i) it induces a shift of the monochromatic modes; (ii) it modifies their stability properties. Our analysis accounts for both effects. Although a detailed study was performed, we only present here the most typical results. These are representative of the evolution of the stability properties of the modes as $R$ is increased. For $R=0$ the mode with maximal gain, the threshold mode, is always (as far as we have seen) stable. In Fig. 2 we show the real and imaginary parts of the eigenvalues for $R=0$. The modes with nonmaximal gain are unstable in one or several directions, as expected (they inherit the stability of the laser-off solution). For $R=0.002$ a pair of new modes is created through a saddle-node bifurcation. While the two modes having the lowest $N$ are stable, the other mode is unstable. In Fig. 3 we show the eigenvalue spectrum for the threshold solution.

For $R\sim 0$ dramatic changes in the stability spectrum are expected and observed. The perturbation introduced by the feedback is a singular one; for $L\to\infty$ a continuous set of allowed perturbations emerges. For finite $L$ these curves are discretized by the boundary conditions. Such lines can be observed in Fig. 3. Note that the isolated points of Fig. 2 are now immersed in two wavy lines with peaks (perturbations with longer decay time) precisely corresponding to the stable perturbations at $R=0$. For example, the relaxation-oscillation modes have now evolved into a full family of modes with small differences in the lasing frequency. The effect of the external cavity is also to lower the damping rate of the perturbations whose excitation frequencies are close to

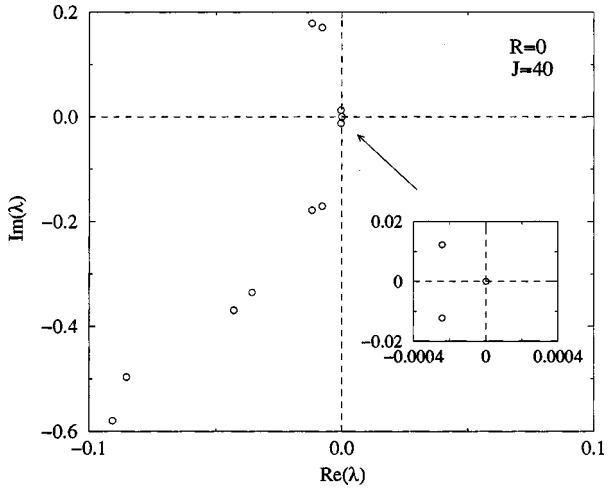


FIG. 2. Eigenvalue spectrum for $R=0$ and $J=40$ for the threshold mode. The inset shows a detail of the marginally stable eigenvalues.

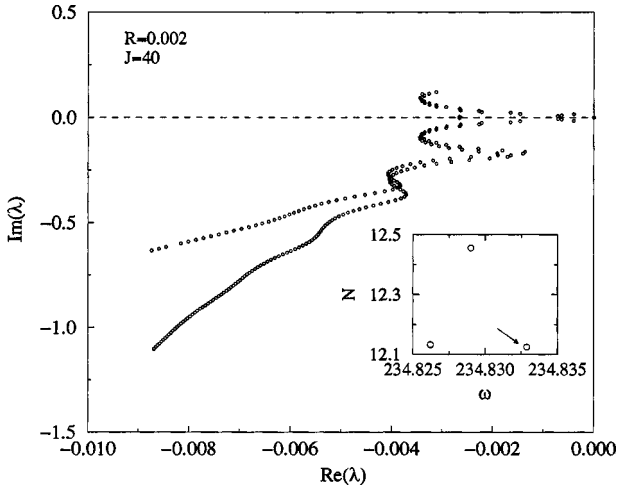


FIG. 3. Eigenvalue spectrum for $R=0.002$. The inset shows the spectrum of monochromatic modes, and the mode under consideration is indicated by the arrow.

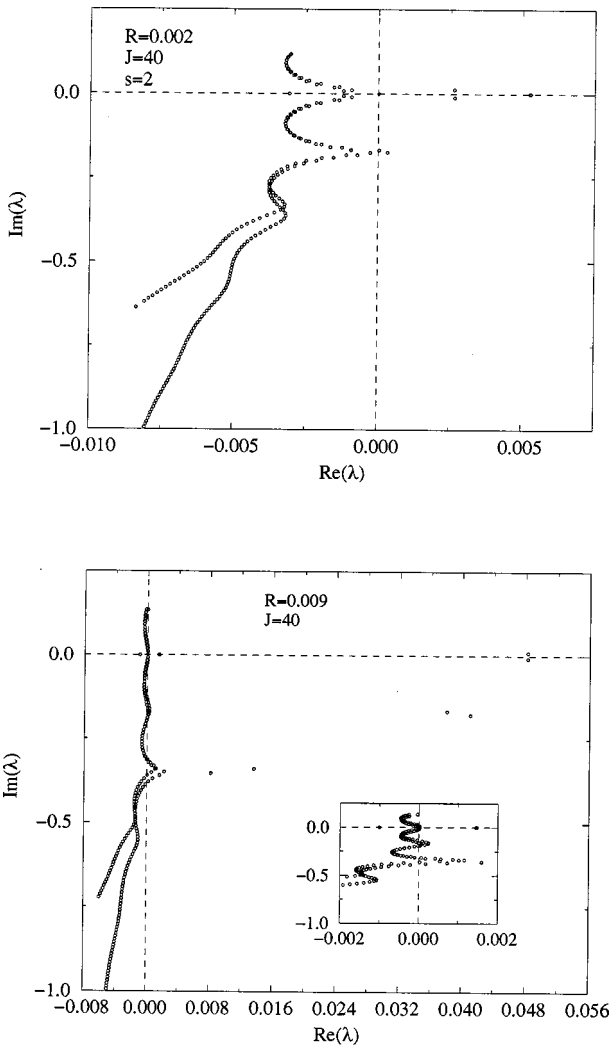


FIG. 4. Eigenvalue spectrum for an unstable mode for different reflectivities $R=0.002$ and $R=0.009$. Note that the degree of instability of this modes increases with $R$. The inset in the lower panel shows a detail of the spectrum near the origin.

the distance between modes of the spectrum obtained for $R=0$.

For $R=0.01055$, the solution with maximal gain as well as the two neighboring solutions are also stable. Nevertheless the stability of these solutions has weakened as consequence of the feedback.

After the metamorphosis of the spectrum, $R>R^*$, it is observed that, while those modes corresponding to local minima of $N$ vs $\omega$ are stable, the rest of the modes are unstable. The most unstable ones are those corresponding to the local maxima of the curve $N(\omega)$. The unstable mode ($R=0.002$) is unstable in several directions, six of them having complex $\lambda$, while the other has real $\lambda$.

The variation of the eigenvalue spectrum of the unstable modes is considered as $R$ is increased. To pursue this analysis we focus our attention on the unstable mode for $R=0.002$ and study the variation of the eigenvalue spectrum of that solution as $R$ is increased. In particular, that spectrum and the one obtained for $R=0.009$ are compared in Fig. 4. As can be seen from the figure, the number of unstable directions is highly dependent on $R$. When $R$ is increased to

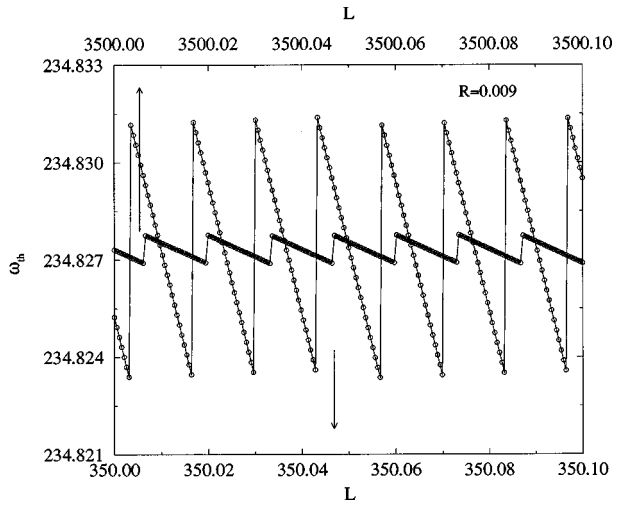


FIG. 5. Dependence of the threshold frequency with $L$ for $R=0.009$. Two different orders of magnitude of $L$ are considered; see the upper and lower scales.

0.009, the peaks that were already present in the curve of $\lambda$ for $R=0.002$ get a more pronounced shape and progressively approach the imaginary axis. As a result, the number of unstable directions with complex $\lambda$ is increased with $R$.

For $R=0.009$ two clearly separated sets of unstable directions differing in the magnitude of the excitation frequency are observed. The excitation frequency of the two sets differs by roughly the frequency separating the modes without feedback.

During the metamorphosis of the spectrum, for $R\sim R^*$, the unstable monochromatic solutions show different spectra of eigenvalues according to whether they have low, moderate, or high carrier density $N$ (which is inversely proportional to the intensity). For low carrier density, the unstable perturbations have $\mathrm{Re}(\lambda)\approx 0.003$, which indicates that the solution is weakly unstable. For moderate $N$, we still observe a wavy curve of $\lambda$. The number of unstable directions has increased as well as the strength of the instability, measured by $\mathrm{Re}(\lambda)\approx 0.11$. We still observe that there are certain excitation frequencies that are clearly more unstable than the others. For large $N$, the solutions are strongly unstable, $\mathrm{Re}(\lambda)\approx 0.4$, for the unstable directions with excitation frequencies associated with the laser cavity. The other solutions, which are also more unstable than in the moderate $N$ case, are highly degenerate in the excitation frequency.

### B. Effect of the external-cavity-length variations

As $L$ is changed, the spectrum of monochromatic solutions is modified mainly through the creation of new solutions. Specifically, our attention is focused on the dependence of the threshold solution and its stability on $L$.

The variations of both the frequency and carrier density of the threshold mode with $L$ are shown in Figs. 5 and 6, respectively. As can be seen from these figures, the dependence of these parameters on $L$ is by no means trivial or expected. Note that for this value of $R$ the spectrum is formed by islands. The variation of $w_{th}$ with $L$ reflects the shift of the monochromatic modes: the island circulates clockwise. Having in mind that (i) the threshold mode is the solution that overcomes the losses with a smaller applied

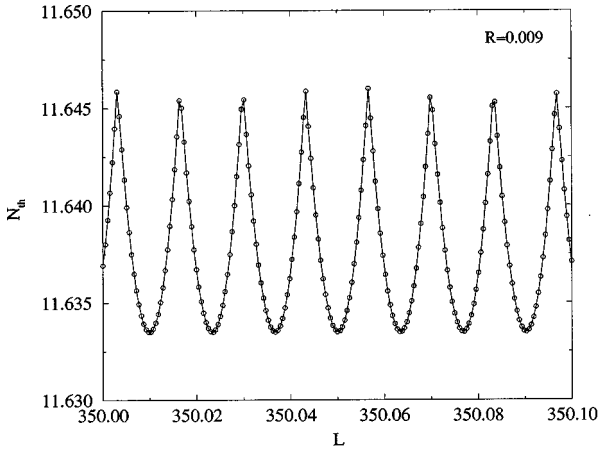


FIG. 6. Dependence of the carrier density of the threshold mode with $L$ for $R=0.009$.

current, and (ii) the material losses are independent of the control parameters ($R$, $L$, and $J$), one could think of $\|N_{th} - \min(N_{th})\|$ as a potential measuring the ability of the system to accommodate such a solution.

As the island rotates, the threshold mode is shifted away from the potential minimum and the mode on the right is shifted towards that minimum. The carrier density of this mode decreases with $L$ until it eventually becomes the threshold solution. The replacement of the threshold mode shows as the jumps in $\omega_{th}(L)$ and the peaks in $N_{th}(L)$.

In Fig. 5 the frequency of the threshold mode as a function of $L$ is shown for ranges of $L$ differing by an order of magnitude. The larger the $L$, the smaller the magnitude of the variation of $\omega_{th}$. This can be understood by considering that, as the number of modes in an island is increased with $L$, the distance between them is reduced. Thus, the $L\rightarrow\infty$ limit of an island of solutions is a circle of modes. In that case the mentioned effect would not be present.

This result is not limited to low $R$ (islands); the same behavior is observed for larger values of $R$ (even above the metamorphosis of the spectrum). The difference is that, when there are no islands, the circulation of modes takes place on a global scale (considering also the upper part of the spectrum), while locally only a shift toward lower frequencies is observed.

The linear stability analysis of the threshold solution is considered. An applied current of $J=4J_{th}$ was used to isolate the effect of $L$ from the variation of effective pumping due to the variation of $N_{th}$. Figure 7 shows the real and imaginary parts of the eigenvalue, with maximal real part corresponding to the threshold solution. Considering the real part of the eigenvalues in Fig. 7 we can see that when the threshold solution switches, the former threshold (smaller $L$ value) is still stable; hence for some values of $L$ there is a multistability of solutions and, presumably, there are hysteresis effects with respect to $L$.

### C. Applied-current-induced effects

In this section we explore the stability properties of the threshold mode as the applied current is varied. Although $J$ does not change the monochromatic spectrum, it does change the intensity of that solution and therefore its stability. Our

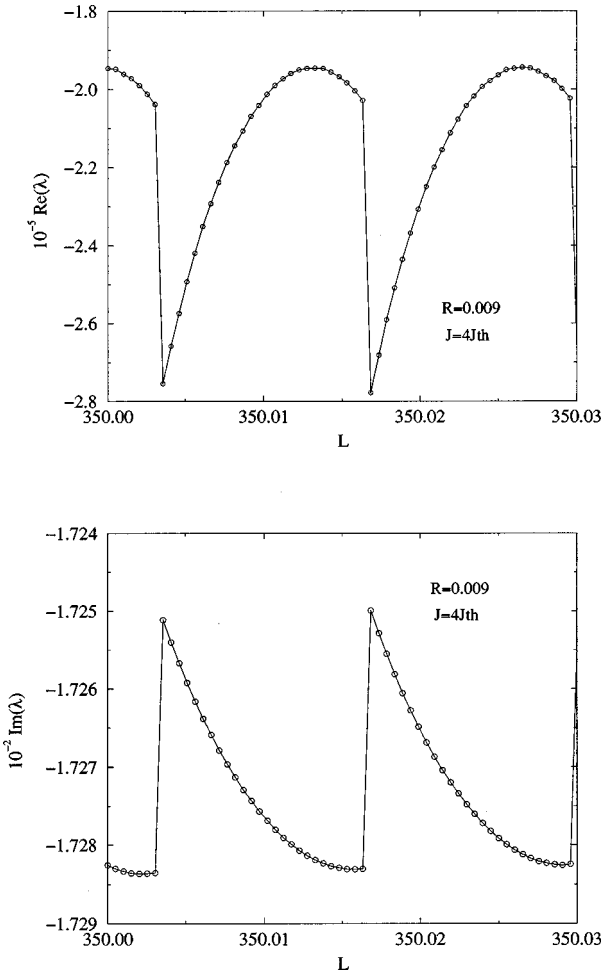


FIG. 7. Stability of the marginally stable eigenvalue of the threshold mode as a function of $L$ for $R=0.009$ and $J/J_{th}=4$.

attention is focused on the threshold mode, and the evolution of the eigenvalue with the largest Re(λ) was studied as $J$ was varied. The stability modes studied always belong to the family of relaxation-oscillation excitations. The analysis is performed for different values of $R$: $R=0$, $R<R^*$, $R\sim R^*$, and $R>R^*$ (in our case, $R^*\approx 0.010\,55$).

For $R=0$ (see Fig. 8), the effect of the applied current is to increase the stability of the threshold mode [lower the maximum Re(λ)] (upper panel), and induces a shift in the frequency of the perturbation (lower panel). Note that these dependences are smooth and monotonic in accordance with what is predicted by simple rate equations [15].

In the upper panel of Fig. 9 we show the Re(λ) plot for $R=0.009$. The existence of the external cavity drastically changes the response of the system to perturbations. In this case, the dependence of Re(λ) on $J$ shows a peaked structure (nonmonotonic), sharply contrasting with what is observed for $R=0$. However, the lasing mode remains stable.

The dependence of Im(λ) vs $J$ for $R=0.009$ (Fig. 9) is also very different from that observed for $R=0$, showing a series of steps at particular values of Im(λ). As $J$ is increased, the perturbation with maximal λ adopts a discrete set of values related to the external cavity. The same kind of dependence is observed for other values of $R$, as long as $R\neq 0$. In particular, the curves are practically the same.

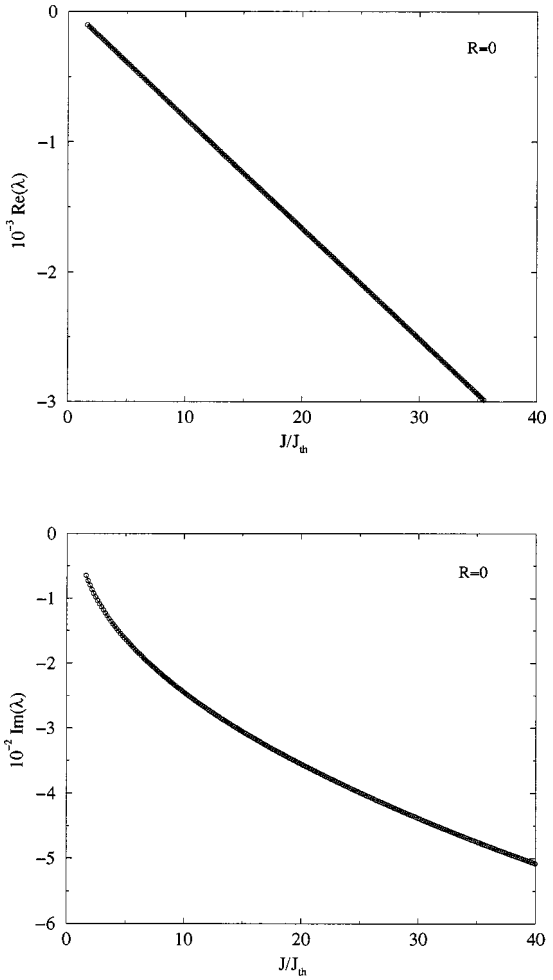


FIG. 8. Real and imaginary parts of the marginally stable eigenvalue of the threshold mode as a function of $J$ for $R=0$.

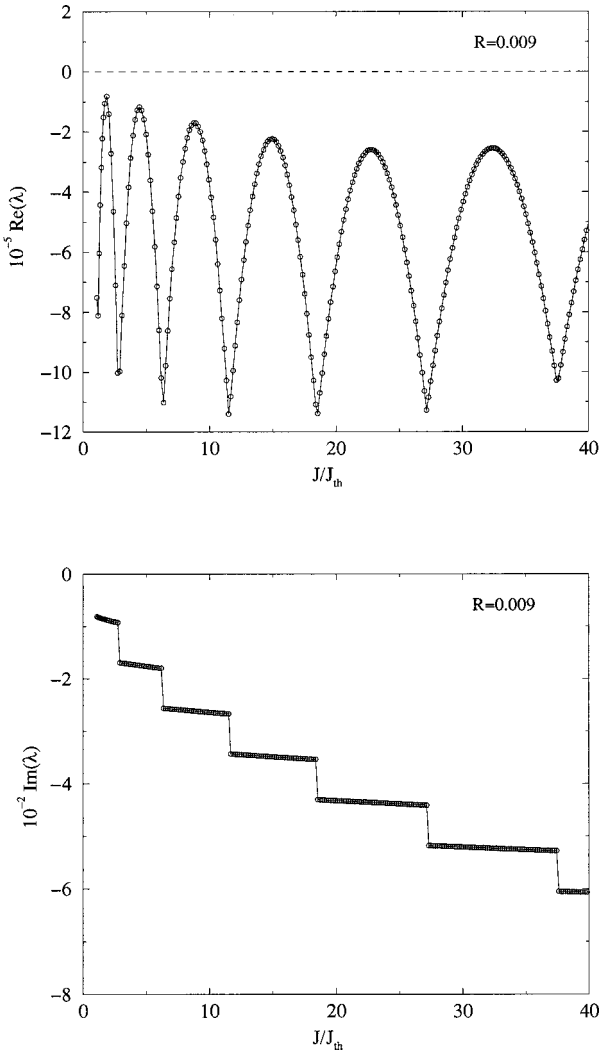


FIG. 9. Real and imaginary parts of the marginally stable eigenvalue of the threshold mode as a function of $J$, below the metamorphosis of the spectrum ($R=0.009$).

It is important to note that the less stable excitation does not identify the same mode in a continuous form. The singularities in the curves of Fig. 9 correspond to the switching of one stable excitation to a different one. Also note that this switching is always accompanied by a sudden increase in the oscillation frequency. Thus the model predicts that the relaxation frequencies will present sudden changes as the current is varied. For very low currents, the less stable (i.e., longer lasting) relaxation oscillation presents low frequencies, increasing the current causes the decay time to increase up to a maximum and then to decrease until a perturbation of higher frequency becomes less stable, dominating the longer-lasting oscillations.

The same analysis is performed for reflectivity values corresponding to the metamorphosis of the spectrum, $R=0.010\,55$. The resulting $\mathrm{Re}(\lambda)$ vs $J$ can be seen in Fig. 10. In this case, the behavior of $\mathrm{Re}(\lambda)$ with $J$ changes qualitatively. The curve still shows the peaked structure, but now there are regions of $J$ where the mode is unstable, giving rise to a Hopf instability where the system suddenly exhibits a frequency equal to $\mathrm{Im}(\lambda)$. The applied current $J$ can give rise to the birth of sustained relaxation oscillations. The magnitude of the excitation frequency of such oscillations is related to the external cavity and is determined mainly by $J$. A peculiarity of the $\mathrm{Re}(\lambda)$-curve is the alternation of regions of stability and instability as $J$ is increased. It must be noted that the Hopf instability marks the starting point of a possible sequence of instabilities that eventually leads to more complicated dynamical states.

Above the metamorphosis, for $R=0.018$, the effects mentioned above are markedly stronger; see Fig. 11. As a result, the mode can be destabilized for smaller $J$.

As $\mathrm{Re}(\lambda)$ can be made arbitrarily small by the effect of $J$, it is clear that the role played by noise (always present in semiconductor lasers) will be very important in this system and the strength of this effect can be controlled by $J$. It can be conjectured from the above-mentioned phenomenology that the noise-induced excitability of this system is very important.

On the one hand, it is known through the experimental classification of the different types of behavior of a double-cavity semiconductor laser [16,11] that, as $R$ is increased, regimes are reached where the system shows noise-induced hopping between several external cavity modes or where the relaxation oscillations are undamped. On the other hand, it is

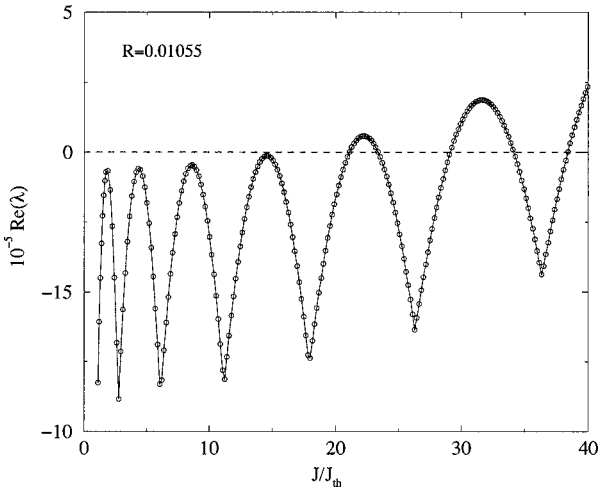


FIG. 10. Real part of the marginally stable eigenvalue of the threshold mode as a function of $J$, during the metamorphosis of the spectrum ($R=0.010\,55$).

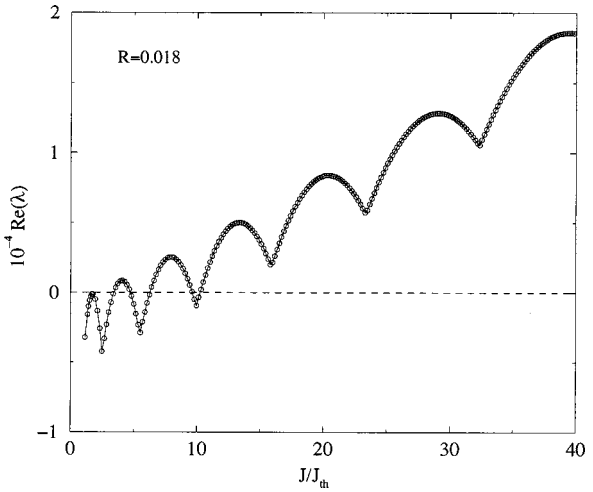


FIG. 11. Real part of the marginally stable eigenvalue of the threshold mode as a function of $J$ once the metamorphosis of the spectrum has taken place ($R=0.018$).

also known that, for moderate levels of feedback, changing the applied current $J$ can reveal other interesting states: the low-frequency fluctuations regime [17,18]. Noise can anticipate the appearance of this current-induced regime, and the undamping of the relaxation oscillations as well as the low-frequency fluctuations regime can be considered as a precursor of the coherence collapse regimes.

Our results are consistent with the phenomenological classification of different regimes present in the system; however, to reach a deeper understanding of the different regimes, a study considering the temporal evolution of the system is needed. We consider that this kind of analysis is a first and necessary step towards a consistent description of the problem for arbitrary $R$.

## VI. CONCLUDING REMARKS

The metamorphosis of the spectrum of monochromatic modes in a semiconductor laser with optical feedback and the stability properties of such solutions were studied as a function of the parameters of the problem, the reflectivity of the external mirror ($R$), the external cavity length ($L$), and the applied current ($J$). The spectrum gradually changes as $R$ is increased from 0 to 1. For low values of $R$, we showed that this transformation proceeds through the formation of ''islands'' of monochromatic modes around each mode of the single laser ($R=0$). Those changes are the consequence of the coupling between the laser and the external cavity and are qualitatively similar to those described by the Lang-Kobayashi equations [2,3].

For larger values of $R$, the merging of the islands takes place giving rise to a more complicated spectrum not describable by the Lang-Kobayashi model. This process is a consequence of the boundary-condition equations and was described in Ref. [9]. Beyond this value of reflectivity, the description of the laser with optical feedback requires a multilongitudinal model, such as the one introduced in [13]. It is important to realize that the need for a multilongitudinal model has been already suggested in at least one experimental work [4] where multilongitudinal operation of a semiconductor laser with optical feedback has been reported beyond the region known as coherence collapse.

The stability properties of the monochromatic solutions were studied by performing different cuts in the parameter space, $(R,L,J)$. When $R$ is increased, the spectrum of eigenvalues of the different modes is strongly affected, reflecting the presence of the external cavity. At a given value of $R$, we found that the number of unstable directions is greatly increased, with the intensity of the lasing mode proportional to $J-N(\omega_i)$. An increase in $R$ drives corresponding increases in the number of unstable eigenvalues and their real parts. In all cases the threshold mode is stable. The variation of the threshold mode and its stability was studied as a function of $L$ for different values of $R$. We found that when $L$ is varied the threshold mode and its eigenvalue with larger real part are shifted in an unusual fashion (Sec. V B). Nevertheless, the threshold mode remains stable. We also show that as $L$ is varied there is a multistability of solutions.

The variation of the marginally stable perturbation with $J$ is shown to be remarkably different, whether $R=0$ or $R\neq 0$. In particular, within the latter case ($R\neq 0$), different behavior is observed, depending on the actual stage of the metamorphosis of the spectrum. Interestingly, the stability type can only be changed for reflectivity values corresponding to the metamorphosis of the spectrum or larger. The stronger the reflectivity of the external mirror $R$, the stronger the dependence on $J$ will be. Note that the destabilization of the threshold mode cannot be recovered by the simpler Lang-Kobayashi model.

The applied current $J$ can induce the birth of sustained relaxation oscillations, whose excitation frequency adopts a set of roughly discrete values related to the external cavity. The role played by noise will be highly dependent on the values of $R$ and $J$. Below the transition, the degree of potentially noise-induced excitability depends on $J$. In this case, although the effect is moderate, depending on the amount of noise, the system can show noise-induced hopping between

the eigenmodes of the stability problem.

For $R$ corresponding to the metamorphosis of the spectrum, we found that for large enough $J$ the dumping of this perturbation can be made arbitrarily small. As a result, the system can be driven into regimes that will be highly susceptible to noise. Above the metamorphosis (large $R$), this dependence on $J$ is highly enhanced, and the mentioned regimes will be reached for smaller $J$.

**ACKNOWLEDGMENTS**

It is a pleasure to thank Gabriel B. Mindlin, Jorge Tredicce, Salvador Balle, and Claudio Mirasso for useful discussions. This work has been supported in part by the University of Buenos Aires (Grant No. Ex-104) and the European Economic Community under Contract No. CI1*CT93-0331.

[1] M. C. Cross and R. C. Hohemberg, Rev. Mod. Phys. **65**, 851 (1993).
[2] J. Mork, B. Tromborg, and P. L. Christiansen, IEEE J. Quantum Electron. **QE-24**, 123 (1988).
[3] I. Fischer, G. H. M. van Tartwijk, A. M. Levine, W. Elsässer, E. Göbel, and D. Lenstra, Phys. Rev. Lett. **76**, 220 (1992).
[4] D. Lenstra, B. H. Verbeek, and A. J. Den Boef, IEEE J. Quantum Electron. **QE-21**, 674 (1985).
[5] I. Fischer, O. Hess, W. Elsässer, and E. Göbel, Phys. Rev. Lett. **73**, 2188 (1992).
[6] J. Sacher, D. Baums, P. Pauknin, Wolfgang Elsässer, and E. O. Göbel, Phys. Rev. A **45**, 1893 (1992).
[7] R. Lang and K. Kobayashi, IEEE J. Quantum Electron. **QE-16**, 347 (1980).
[8] M. H. Rose, M. Lindberg, W. W. Chow, S. W. Koch, and M. Sargent III, Phys. Rev. A **46**, 603 (1992).
[9] A. A. Duarte and H. G. Solari, Phys. Rev. A **58**, 614 (1998).
[10] G. P. Agrawal and N. K. Dutta, *Long-Wavelength Semiconductor Lasers* (Van Nostrand Reinhold, New York, 1986).
[11] Guido Henri Maria van Tartwijk, Ph.D. thesis, Vrije Universiteit, 1994 (unpublished).
[12] S. Balle, Opt. Commun. **119**, 227 (1995).
[13] A. A. Duarte and H. G. Solari, Opt. Commun. **144**, 99 (1997).
[14] W. W. Chow, S. W. Koch, and M. Sargent, *Semiconductor-Laser Physics* (Springer, Berlin, 1994).
[15] H. G. Solari, M. A. Natiello, and B. G. Mindlin, *Nonlinear Dynamics. A Two Way Trip from Physics to Math* (IOP, Bristol, UK, 1996).
[16] R. W. Tkach and A. R. Chraplyvy, J. Lightwave Technol. **LT-4**, 1655 (1986).
[17] M. Giudici, C. Green, G. Giacomelli, U. Nespolo, and J. Tredicce, Phys. Rev. E **55**, 6414 (1997).
[18] M. Eguia, B. G. Mindlin, and M. Giudici, Phys. Rev. E **58**, 2636 (1998).